APPLICATION NOTE

CELLREV

Short and Sweet: AggreGuard™ facilitates reduced upstream process optimisation and increases eGFP-production post-transduction

Scott Kerridge, Esha Singh, Azzeldin Madkour, Laura Duffy, Martina Miotto and Francois Taute*

Abstract

Cell-to-cell adhesion is the main driver of cell clumping and microcarrier aggregation in suspension-based agitated bioreactors. Cell clumping is an intrinsic biological trait to facilitate the main cellular function of tissue formation, facilitated by the extracellular matrix which consists of proteins and other biomolecule species. The function of the extracellular matrix includes structural support for cells, a transduction pathway for biomechanical cell signals as well as an exclusion barrier to shear damage and unwanted interactions with foreign matter particles. Cell clumping decreases cell culture homogeneity, resulting in decreased cell viability and productivity as the aggregates reach biological diffusion limits. Process control, cell line engineering and media formulation approaches can reduce cell-to-cell clumping, at the cost of extracellular matrix function, often with significant resource investment (***time > money > labour***) in upstream process development, usually the least costly unit operations in global process development and manufacturing pipelines. CellRev tested a hypothesis: reducing cell-to-cell adhesion with AggreGuard™ in a representative upstream bioprocess can improve the viral titre while maintaining cell culture homogeneity without cell line engineering or media formulation. This hypothesis was evaluated in 125mL disposable Corning® spinner flasks using an enhanced green fluorescent (***eGFP***) protein expressing adeno associated viral vector to transduce Vero cells, mimicking a viral infection. Results showed that a reduction in cell-to-cell adhesion with AggreGuard™ (i) increased eGFP expression ~3-fold; (ii) resulted in a visually a more homogenous cell culture; and (iii) yielded a 1.5-to-2-fold more viable cells harvest at process end.

Introduction

The development of therapeutic molecules is a protracted challenging process, requiring scientific validation from a basic scientific understanding through developing a biomanufacturing strategy while navigating (pre)clinical trials, regulatory requirements and post-commercialisation pharmacovigilance. The typical viral vaccine candidate process can take 12 – 15 years from preclinical phase to pre-commercialisation[1,2], where the viral vaccine candidate may never make it to market as the success rate is expected at 10 – 15%. Failure to reach market is usually attributed to two factors: (i) inefficacy and safety concerns in human trials or (ii) an inability to meet minimum scaling and economics of manufacturing criteria.

Vaccines are typically a high-volume product, requiring manufacturing to produce a few hundred million doses per annum for rollout to ensure adequate disease management and control. Manufacturing requires a bioprocess which is robust with low lot-to-lot variation, scalable to drive down cost of production per volume and meet clinical demand. The cost of manufacturing[3,4] in a typical viral vaccine bioprocess is distributed between upstream (**~25%**) and downstream (**~75%**) processes, where challenges in developing an upstream process (**USP**) impacts the full manufacturing value chain, not only impacting development cost and timelines but also jeopardising envisioned commercialisation.

Challenges in USP development are driven by intrinsic cellular behaviour in tissue formation, facilitated by cell-to-cell attachment (**C2CA**). The intrinsic C2CA does not significantly affect planar cell culture (i.e., T-flask, multilayer culture vessels), however in suspension-based culture vessels (i.e., stirred tank

bioreactors) cells readily form unwanted clumps[3,5]. Cell clumping occurs for most single cell suspension or anchorage dependent cells grown on microcarriers (**MCs**), resulting in a less homogenous cell culture environment with inefficient mass transfer leading to biochemical gradients. A loss in culture homogeneity is associated with cell productivity variation as well as increased cell-derived product quality variation. Batch loss occurs when the average diameter of C2CA induced clumps or aggregates exceed 350µm. The extracellular matrix[6,7] (**ECM**) is a complex mixture of biomolecules (*i.e. proteins, extracellular nucleic acids*) serving as a scaffold for cells to adhere to as well as to each other, additionally acting as a mechanical stress modulator (*i.e., shear, compression, elongation*) and exclusion barrier[6] to macromolecules and larger particles (*i.e. viruses, bacteria*).

A bioprocessing approach to control C2CA induced clumping is through process control (*pH, temperature, dissolved oxygen and agitation*), usually through agitation-based protocols to improve mixing in the bioreactor. There is a balance required between agitation, shear stress experienced by the cells and cell health as well as productivity to ensure the process is scalable. A cellular response to increased shear stress is ECM secretion[8,9] (*cell type dependent*), counterproductive to process control. Alternative routes to prevent cell clumping is cell line engineering and adaptation or media formulation – time consuming and costly exercises which do not always translate well from planar to suspension culture.

In this application note we showed how AggreGuard™, a blend of ECM-specific enzymes, enabled a more controlled and homogenous USP cell culture environment without extensive optimisation of process parameters in spinner flasks. This was evaluated using a Vero cell-based MC model in spinner flasks, with an adeno-associated viral vector (***AAV***) expressing enhanced green fluorescent protein (***eGFP***) used to mimic viral infection. Results showed that if C2CA was enzymatically controlled with AggreGuard™, there was (i) an overall ~3-fold increase in eGFP signal; (ii) a more homogenous cell culture environment and (iii) a 1.5-to-2-fold more viable cells retrieved from MCs at the process end. The addition of AggreGuard™ allowed for a facile process to be established without the need to use process control to improve overall cell productivity.

Materials and Methods

The summarised materials used in this study can be found in Table 1. A brief discussion on methods follows.

Table 1: Materials used for this study

Components	Description
Cell line	Vero cells (ECACC Cat No: 84113001)
Microcarrier type	SoloHill® Plastic Plus Microcarriers (360cm²/g; Sartorius, Cat. No. PP-221-020)
Composition of medium	DMEM/F12 (Gibco) enriched with 10% FBS (Gibco) and 1% Penicillin-Streptomycin (Gibco).
Dissociation agent	Gibco™ TrypLE™ Express Enzyme
Cell Culture Flask	175 cm² culture flasks (Greiner Bio-One Cat. No. 660175).
Spinner Flask	125 mL; Corning disposable spinner flask (Cat. No. CLS3152
AggreGuard™	Developed by CellRev
Adeno-associated Virus Vector	AAV/DJ-CMV-eGFP (VectorBiolabs; Cat. No. 7101; Lot:230320-240228)

Cell Culture: Vero cells were grown in DMEM/F12 supplemented with 10% FBS and 1% Penicillin-Streptomycin, maintained in 175 cm² culture flasks before being seeded onto microcarriers in spinner flasks (Table 1).

Microcarrier Protocol Development: The SoloHill® Plastic Plus (SPP) microcarriers (MC) were prepared as per the manufacturer's guidelines (washing, autoclaving) and equilibrated for 30 minutes using cell culture media. Following equilibration, 1g of the SPP MCs were transferred to each 125 mL Corning® disposable spinner flasks, followed by seeding of Vero cells (10 000 cells/cm^2). The cell attachment phase was 5h of intermittent agitation (25 min rest; 5 min agitation) using a 2mag bioMIXdrive agitation system in a humidified incubator at 37°C, 5% CO_2. After successful cell attachment, medium was added to a final volume of 40 mL and agitation adjusted to 30rpm for the rest of the culture duration. An experimental design for the spinner flasks required a cell growth control (No AAV addition, No AggreGuard™ addition); a ***AAV*** control (***AAV*** = AAV addition, No AggreGuard™ addition) and a AggreGuard™ containing flask (***AG-AAV*** = AAV addition, AggreGuard™ addition). AggreGuard™ was added to the appropriate spinner flask on process day 3, when the first signs of C2CA induced cell-MC aggregation was observed as doublets or triplets. AggreGuard™ addition timing and dosage maintenance was determined in optimisation experiments. Partial media exchanges were done every 48h, unless noted otherwise, for all flasks. The total culture duration was 14 process days, with 9 days post AAV transduction, with cell harvesting from the MCs done using 100% TrypLE.

AAV Transduction: The multiplicity of infection (MOI) was determined at 10^3 for 20h in optimisation experiments (24 well) to determine peak of eGFP fluorescence. The MOI protocol was transferred and evaluated on the MC protocol and no adaptation was found to be required. Prior to transduction, the cell densities in each spinner flask were adjusted to equal densities using the NucleoCounter. A ~85% media exchange was done in all spinner flasks, followed by AAV addition to the AAV control and the AG-AAV flasks. A further ~85% media exchange was done 20h post transduction. The media exchange protocol proceeded as normal.

Culture Monitoring: Daily sampling was performed to qualitatively assess cell attachment on microcarriers (brightfield microscopy), cell-surface coverage on the microcarriers and microcarriers aggregation status. Samples were collected periodically for cell counting (NucleoCounter NC202, lysis buffer A method) and fluorescent Live-Dead staining (Hoechst, Propidium Iodide) using a Cytation 5 (BioTek) imaging system. Daily metabolite (glucose, lactate) levels were assessed using handheld electrochemical biosensors. Protein content was determined using a BCA assay (Pierce BCA Protein Assay Kit, Thermofisher) on a VarioSkan LUX Multimode plate reader. eGFP signal was also quantified using a Varioskan LUX Multimode plate reader (Thermofisher).

Results and Discussion

Cell culture parameters (*proliferation, C2CA-mediated aggregation, cell harvest, cell viability*): Vero cells were seeded onto the SPP MCs where qualitative microscopy assessment (***Fig. 1***) was used to determine overall C2CA-induced aggregation. AggreGuard™ (***AG-AAV***) was added to a spinner flask on process day 3 (*confluency ≈ 60%*), followed by AAV-mediated transduction on process day 5. The remaining spinner flasks received no AggreGuard™ and only transduced with (***AAV***) on process day 5, or no AggreGuard™ and no transduction (***Control***). The spinner flasks without AggreGuard™ showed the start of aggregation by process day 3 (*doublets, triplets, and larger clusters*) which resulted in severe aggregation by process day 9 and increasing amounts of detached cells and cell debris being observed throughout the process. Aggregation was minimally observed or absent in the spinner flask treated with AggreGuard™, where there was comparatively less detached cells or cell debris.

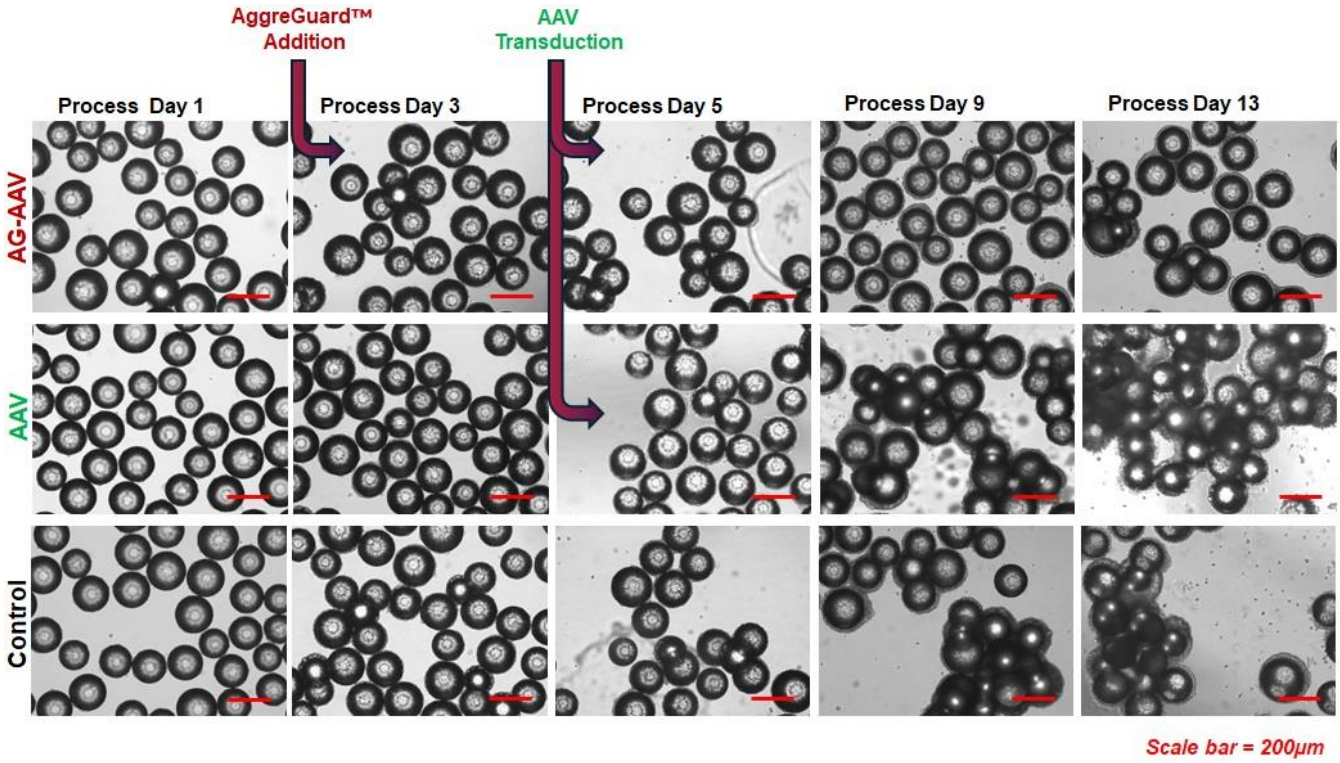

Figure 1: Micrographs showing the progression of the three processes over a total duration of 13 days. AggreGuard™ (***AG-AAV***) was added to one spinner flask on the third process day, followed by AAV transduction in the AggreGuard™ treated flask (***AG-AAV***) as well as a flask without AggreGuard™ treatment (***AAV***). A third spinner flask served as a double negative control. AggreGuard™ enzymatically controlled C2CA over the full process duration.

Daily cell counts (***Fig. 2A***) showed there was no difference in cell counts between the spinner flasks until process day 9, where the AggreGuard™ treated flask (***AG-AAV***) showed an increase in cell number. At process end, day 13, cells were harvested using TrypLE with viable cell recovery (***Fig. 2B***) ~55% for control, ~120% for ***AAV*** and 98.5% of ***AG-AAV***. A NucleoCounter total cell count was done to determine cell counts prior using TrypLE to recover the cells (***Fig. 2B, Pre-Harvest***) and a cell count after the cells have been processed (***Fig. 2B – Post-harvest***). The cell recovery for the AAV-spinner flask is attributed to inaccurate cell counting from the severe aggregation status, making it difficult to prepare single cells suspensions. Overall, when total live cell yield is considered, the addition of AggreGuard™ facilitated a ~2-fold increase (***AG-AAV:Control***) and ~1.4-fold increase (***AG-AAV:AAV***) when compared to other conditions. The addition of AggreGuard™ promoted better tissue culture conditions by improving overall better MC-cell homogeneity in suspension which facilitates improved mass transfer and mixing conditions. The improved mixing is also a contributing factor to a more facile cell harvest with a higher overall live cell yield.

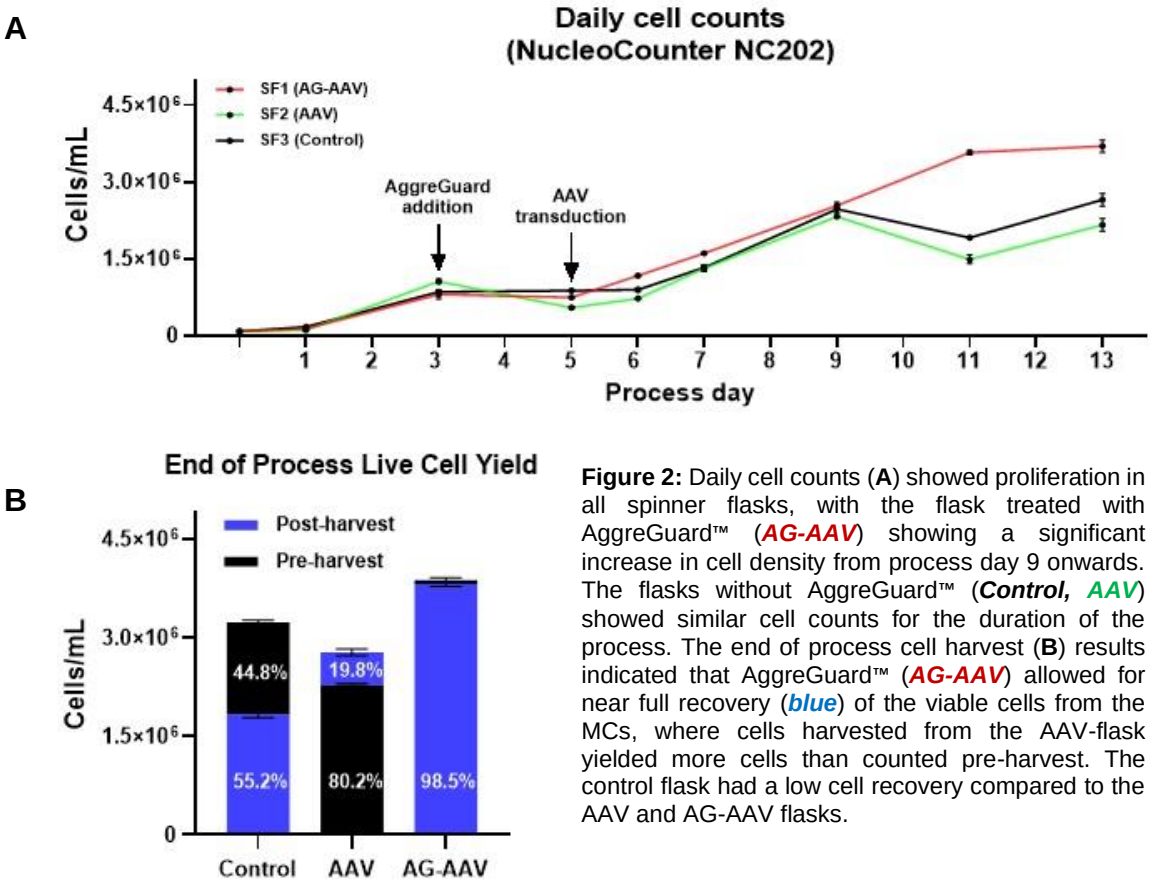

Figure 2: Daily cell counts (**A**) showed proliferation in all spinner flasks, with the flask treated with AggreGuard™ (***AG-AAV***) showing a significant increase in cell density from process day 9 onwards. The flasks without AggreGuard™ (***Control, AAV***) showed similar cell counts for the duration of the process. The end of process cell harvest (**B**) results indicated that AggreGuard™ (***AG-AAV***) allowed for near full recovery (***blue***) of the viable cells from the MCs, where cells harvested from the AAV-flask yielded more cells than counted pre-harvest. The control flask had a low cell recovery compared to the AAV and AG-AAV flasks.

Fluorescent staining of the cells on the MCs was performed at the end of process together with visual inspection (***Fig. 3***). The AggreGuard™ treated flask (***AG-AAV***) showed lower propidium iodide signal intensity than the other conditions. Naked-eye assessment of the bottom of the spinner flasks was done after allowing the MCs to settle for 2 minutes once removed from agitation. The MCs appeared more disperse and individually defined for ***AG-AAV***, with no visible aggregation. Severe aggregation and tissue-like formation was observed for ***AAV*** and control. The fluorescence microscopy and visual results are in line with the cell brightfield microscopy (***Fig.1***) and cell count (***Fig. 2***) data, showing increased cell culture homogeneity (≈ ↓aggregation) leading to more viable cells recovered. In particular, the propidium iodide intensity in the aggregated spinner flasks (***Fig. 3 - Control, AAV***) is the most intense between MCs where C2CA is the most prominent, demonstrating that cell-MC aggregates do not require a significant clustering size to already show cell death.

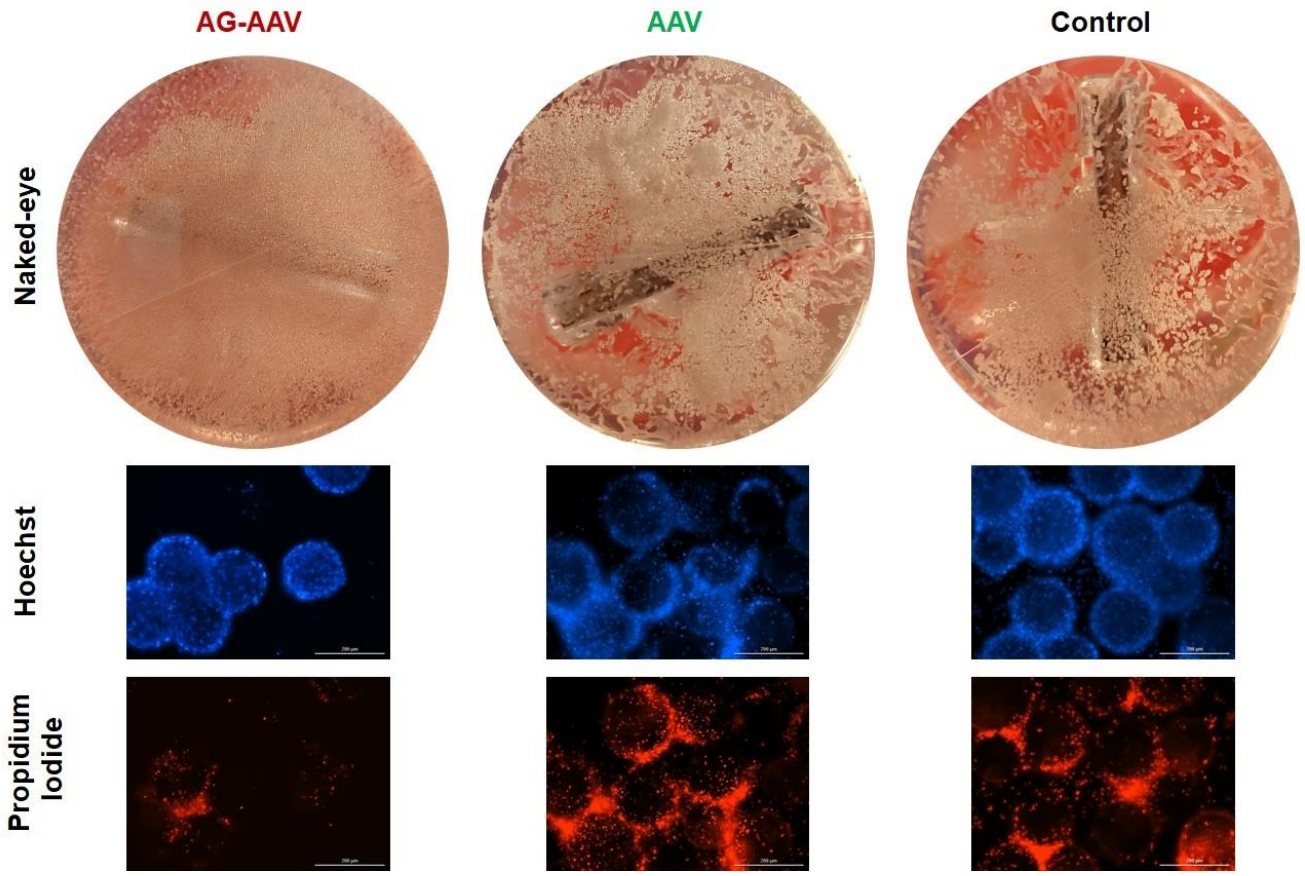

Figure 3: End of process fluorescent staining was performed (**Hoechst, Propidium iodide**) for a qualitative evaluation of dead cells in the spinner flasks prior to their harvest from the MCs. The intensity of the propidium iodide stain was significantly lower for the AggreGuard™ (***AG-AAV***) treated spinner flask than for the ***AAV*** and control flasks. Visual analysis of the aggregation status in the flasks indicated that the cell culture was more homogenous with highly dispersed single MCs covered with cells when treated with AggreGuard™ (***AG-AAV***), whilst aggregation and clumping was evident in the other spinner flasks (***AAV, control***).

The impact of AggreGuard™ and the MC aggregation status on eGFP fluorescence signal intensity: The eGFP signal was measured, starting 24 hours post-transduction, until a decline in the eGFP signal intensity was observed (process end). The eGFP signal was normalised to the total cellular protein, as eGFP is an intracellular product and would be proportionally reflected in a total protein determination. The AggreGuard™ treated spinner flask (***Fig. 4A, AG-AAV***) showed a faster increase in total signal over 24 hours, with a further increase in eGFP signal from process day 7 to 9. The untreated spinner flask (***Fig. 4A, AAV***) comparatively showed a reduced increase in total eGFP signal over the process duration, especially when total fold increase (***Fig. 4C***) was calculated using process day 6 AAV signal as a reference point, with ***AG-AAV*** showing ~20 (***AG-AAV process day 7***) to ~25-fold (***AG-AAV process day 9***) increase. AAV showed ~5-fold change at similar timepoints. When total area under the curve (***Fig. 4B – A_{Total}***) was calculated, a ~3-fold increase in eGFP signal was found for ***AG-AAV:AAV***.

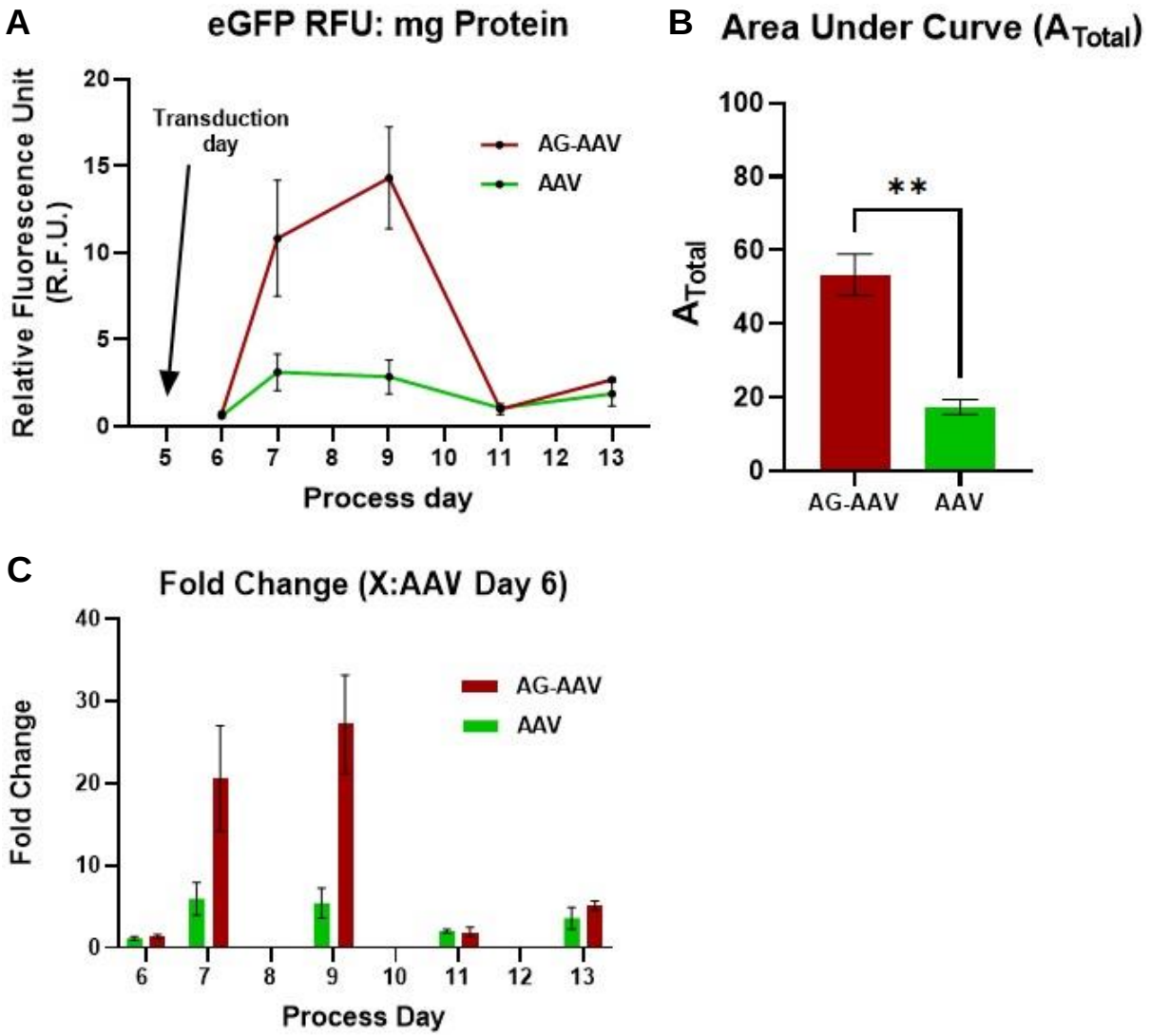

Figure 4: The normalised eGFP fluorescence intensity (A – eGFP R.F.U.: mg Protein) showed that the addition of AggreGuard™ (***AG-AAV***) resulted in a more intense and sustained fluorescence signal, compared to the spinner flask which did not have AggreGuard™ (***AAV***). The eGFP signal for both conditions had a significant loss of intensity by process day 11. When total area under the curve (B) was calculated for (A), there was a ~3-fold difference between ***AG-AAV*** and ***AAV***. The fold increase (C) for both eGFP signals (***AG-AAV, AAV***) were compared to the ***AAV*** signal generated on process day 6, where ***AG-AAV*** had a significant increase of ~20-fold by process day 7 and ~25-fold by process day 9. The fold increases for process day 7 and 9 was significantly lower for ***AAV***, ~5-fold on both days. X – all conditions used to compare to ***AAV*** day 6.

The increase in total eGFP signal when AggreGuard™ is present is attributed to (i) the cell-MC culture being more homogenous and allowing for improved mixing and (ii) the formulation of AggreGuard™ targets the extracellular matrix, an exclusion barrier, and makes this more porous. Furthermore, when Fig. 1-3 are considered, the presence of AggreGuard™ promotes a higher viability for cells in culture. When C2CA-induced MC aggregation occurs (***Fig. 1, Fig. 3 – Control, AAV***) there is a significant increase in cell death. The cell death observed for the control and ***AAV*** does not appear to originate from a metabolic origin as the glucose consumption and lactate production (***Fig. 5***) did not show any significant variation between all experimental conditions. When the daily cell counts (***Fig. 2A***) is taken into consideration, it should be noted that the NucleoCounter protocol for cell counting is different to the protocol for a LIVE:DEAD assay. During cell counting on the NucleoCounter, a sample is exposed to a lysis buffer to extract the nuclei from the cells. Cells which have recently died or are already showing

permeability to propidium iodide (***Fig. 3***) will have intact nuclei or ssDNA, adding to the total cell count for the day.

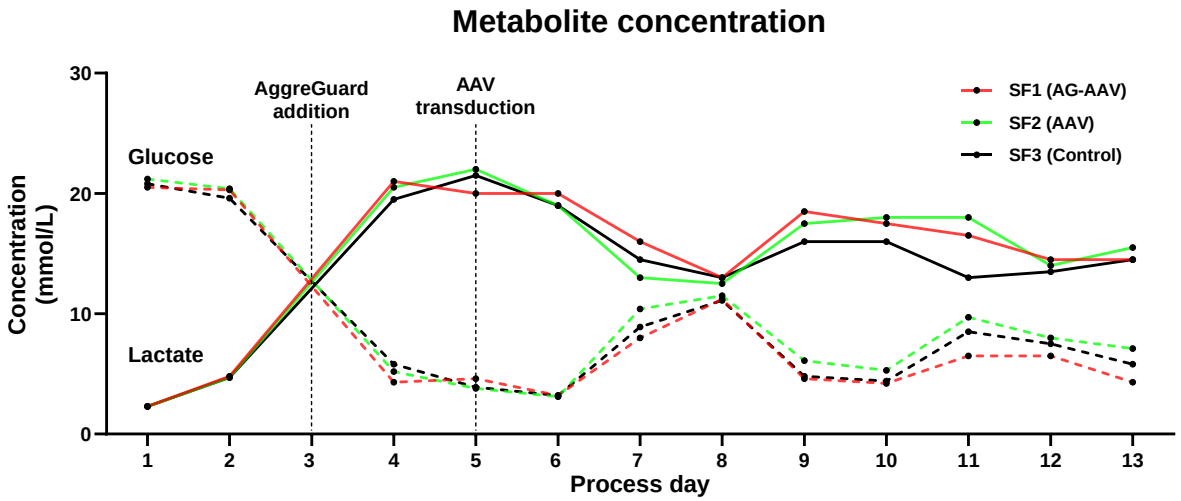

Figure 5: The glucose consumption and lactate production did not vary significantly for all experimental conditions during the whole process duration.

During cellular events such as viral infection or AAV-associated transduction, the intracellular immune response is to expel the foreign nucleic acids through exocytotic pathways or activate programmed cell death[8]. eGFP has mild cytotoxicity[10] towards mammalian cells, through oxidative stress mediated pathways, present as an intracellular protein in this study. The cytotoxicity of eGFP contributes toward overall increased cell death, especially more impactful if cells are already stressed as C2CA-MC aggregates (***Fig. 3 - AAV***), where the presence of AggreGuard™ prevented excessive cell death indirectly by facilitating more homogenous cell culture conditions (***Fig. 1, Fig. 3 – AG-AAV***), in particular improved mixing which promotes improved nutrient-waste exchange between the cells and the media. Overall, AggreGuard™ facilitated higher cell productivity for producing eGFP (***Fig. 4***).

Conclusion(s)

The aim of this study was to determine whether AggreGuard™ has the potential to improve cellular productivity in a typical bioprocess experiment in spinner flasks, by enzymatically controlling C2CA-mediated MC aggregation. An eGFP-AAV was used to simulate a viral infection with subsequent observation on the differences in eGFP signal intensity with and without AggreGuard™. The results from this study show that AggreGuard™ successfully:

- Maintained a more homogenous cell culture without excessive process parameter optimisation
- There was ~2-fold more viable cells retrieved at end of the process with high viability (~98%)
- The overall eGFP signal was ~3-fold higher when compared to control conditions
- The eGFP signal reached peak intensity fast and maintained peak intensity for longer when compared to control conditions

The use of AggreGuard™ allowed for reduction and more control of ECM-components, in a dose-dependent manner, without the need to do multifactorial process control optimisation.

References

1. Krammer, F. “SARS-CoV-2 Vaccines in Development.” 2020. *Nature*, 586:516-527, https://doi.org/10.1038/s41586-020-2798-3
2. MacPherson, A., et al. “Probability of Success and Timelines for the Development of Vaccines for Emerging and Reemerged Viral Infectious Diseases.” 2020. *Annals of Internal Medicine*, 174, DOI:10.7326/M20-5350
3. Buckland, B. et al. “Vaccine process technology – A decade of progress.” 2024. Biotechnology and Bioengineering, 121:2604-2635, DOI: 10.1002/bit.28703
4. Feddema, J.J., et al. “Upscaling vaccine manufacturing capacity – key bottlenecks and lessons learned.” 2023. *Vaccine*, 41:4359-4368, DOI: 10.1016/j.vaccine.2023.05.027
5. Kiesslich, S and Kamen, A.A. “Vero cell upstream bioprocess development for the production of viral vectors and vaccines.” 2020. *Biotechnology Advances*, 44:107608, https://doi.org/10.1016/j.biotechadv.2020.107608
6. Dzobo, K. and Dandara, C. “The Extracellular Matrix: Its Composition, Function, Remodeling, and Role in Tumorigenesis.” 2023. *Biomimetics*, 8(2):146, https://doi.org/10.3390/biomimetics8020146
7. Franchi, M. “Extracellular matrix biomechanical roles and adaptation in health and disease.” 2023. The FEBS Journal, 291(3):430-440.
8. Espina, J.A., et al. “Response of cells and tissues to shear stress.” 2023. *J Cell Sci*., 136(18):jcs260985, DOI:10.1242/jcs.260985
9. Berdiaki, A. et al. “Extracellular Matrix Components and Mechanosensing Pathways in Health and Disease.” 2024. *Biomolecules*, 14(9):1186, https://doi.org/10.3390/biom14091186
10. Ganini, D. et al. “Fluorescent proteins such as eGFP lead to catalytic oxidative stress in cells.” 2017. *Redox Biology*, 12:462-468, https://doi.org/10.1016/j.redox.2017.03.002